Available online at www.scholarsresearchlibrary.com

Scholars Research Library

Archives of Applied Science Research, 2014, 6 (2): 48-60
(http://scholarsresearchlibrary.com/archive.html)

ISSN 0975-508X
CODEN (USA) AASRC9

Microstructural parameters affirm eutectic composites terminal nature

B. L. Sharma[1], R. K. Bamezai[2], D. S. Sambyal[2], Sham Lal[2] and Deepa Manhas[2]

[1]Yogananda college of Engineering and Technology Gurha Brahmana (Patoli) Akhnoor Road, Jammu
[2]Department of Chemistry University of Jammu, Jammu

ABSTRACT

The lamellar spacing changes among microstructural parameters of any two eutectic phases are related to their entropies of fusion. An immense systematic series of investigation and observation thereof, predicts the terminal nature of both transparent and opaque binary eutectic systems. Experimental evidences are obtained for theoretical shapes of the lamellar solidus-liquidus interfaces, for the movement of lamellar-faults and for the development of low-energy solidus-solidus boundaries between the lamellae. A comprehensive explanation is presented to account for the regular, irregular and complex regular structures which are found in an experimental series of eutectic systems. In the domain of present probe, an important evidence is obtained that reflects the lamellar eutectic structure to be less regular compared to rod eutectic structure.

INTRODUCTION

According to aspects of solid state chemistry, homogeneous solidus solutions are usually formed from different solid components belonging to the same space group, whereas heterogeneous solidus solutions result-in when the components differ in their space groups. In view of the aforementioned impelling evidential inference, eutectic composites are heterogeneous systems consisting of two or more solidus phases differing in space groups which are in equilibrium with the single liquidus phase as established from the study of phase diagrams of multicomponent systems experiencing lowest liquidus point.

The growth habits of the solid components from their respective molten phases are related to the generalization interconnecting, crystallite boundary shape and entropy of fusion [1-5]. Experimental observations are such that classify single phase materials into two groups in view of their solidification characteristics. Those that grow as faceted crystals and those that grow as nonfaceted crystals. The crystallite habits of single phase materials are comprehensively explained by thermodynamic reasoning that the type of growth depends on a factor α, the entropy of fusion in dimensionless units, obviously $\alpha = \xi\left(\frac{\Delta S_F}{R}\right)$ where $\Delta S_F / R$ is entropy of fusion in dimensionless units and ξ is a crystallographic factor which is less than and almost one, and represents the fraction of total number of neighbours situated in the newly formed crystal layer[1-3].

Most non-metals have high entropies of fusion ($\alpha > 2$) and grow with crystalline facets. Most metals have low entropies of fusion ($\alpha < 2$) and grow almost isotropically with no facets. Thus eutectics may be classified into three groups in a similar manner. Those in which both phases have low entropies of fusion grows with nonfaceted-nonfaceted (nf-nf) structured crystals, those in which one phase has high and the other phase has a low entropy of fusion exhibit faceted-nonfaceted (f-nf) and those in which both the phases have high entropies of fusion express faceted-faceted structured crystals. Lamellar or rodlike structures are formed in systems in which both phases have low entropies of fusion. In these alloys, dendrites of either phase may be formed, when the alloy is rich in the relevant component. Examples are Pb-Sn, Sn-Cd, Pb-Cd, Sn-Zn. Irregular or complex regular structures are formed in alloys in which one phase has a high entropy of fusion ($\alpha>2$) and the other has a low entropy of fusion ($\alpha<2$).

Examples are Pb-Bi, Sn-Bi, Cd-Bi. When the alloys are rich in the low entropy of fusion phase, dendrites are formed; when the alloys are rich in the high entropy of fusion phase, faceted primary crystals are produced. These crystals are sometimes called hoppers or pseudodenrties. In this work the term dendrite will only be used to describe nonfacted primary crystals. Dendrites are not formed during solidification in high entropy of fusion single-phase materials.

The third group of eutectics includes alloys in which both phases have high entropies of fusion ($\alpha>2$) and each phase grows with a faceted solidus-liquidus interface, since most metals do not have high entropies of fusion, metallic examples in this eutectic group are rare. However, they may occur between some intermetallics and semiconductors or semimetals such as silicon, germanium and bismuth. Attempts have been made to study eutectic solidification visually by watching the growth process. Since metals are not transparent, the observations have to be made on their external surfaces. This difficulty can be overcome by using transparent analogs of the metallic systems. Most single-phase compounds have entropies of fusion greater than 2 and so grow as facted crystals. Recently organic materials with entropies of fusion less than 2 were investigated. These materials grow in exactly the same way as the low entropy of fusion metals.

MATERIALS AND METHODS

2.1 purification and physical parameters of materials

An interpretation of homogeneous materials′ purity implies that organic materials are less pure and even small portion of soluble impurities can essentially adverse the impact of anisotropic growth in disseminating lamellar structure. To minimize the impurity in effect, analytical reagents especially of BDH Ltd; Alfa Aesar and Merck were the preferential and pronounced selection in the present probe. Thermal analysis (Linseis STAPT-1000) and thaw-melt techniques were adopted in ascertaining the purity of 99.9% homogeneous organic materials, namely, benzoic acid; naphthalene; camphor; camphene; acenaphthene; vanillin and 99.999% pure metals, viz., Sn, Cd, Pb and Bi. The fusion temperatures and enthalpies of fusion of the homogeneous materials, obtained by aforementioned experimental techniques were found conforming to the literal values [6], yielding their dimensionless entropies of fusion, α defined in the introduction section.

2.2 preparation of eutectic composite materials

Eutectic composite materials of binary organic vanillin-acenaphthene; naphthalene-acenaphthene; benzoic acid-salicylic acid; benzoic acid-camphor and metallic systems Sn-Cd, Pb-Sn, Pb-Bi and Sn-Bi were prepared from their constituent materials taken in proportions as specified for their respective compositions in the literature [7-9]. The homogeneity of binary eutectic mixtures at each composition was attained by heat-chill method. The purity and the composition of the eutectic materials were ascertained by thaw-melt technique and thermal analysis.

2.3 growth habits

2.3.1. anisotropic growth

The significance of the anisotropic axial growth implies that the growth direction is quite large along the selected axis compared to its lateral axes. The experimental setup to achieve this particular growth from molten states of binary composite phases was illumed recently [1,10] with the difference that the water reservoir was considered suitable for the transparent binary organic composite materials and silicone oil reservoir for the opaque binary metallic systems owing to the temperature difference between two kinds of composite systems, namely, low temperature transparent materials up to 423K and high temperature opaque composite materials up to 650 K.

2.3.2. isotropic growth

The physical understanding of the isotropic (directionless) growth implies that the solidification process of binary composite phases from molten state must manoeuvre the mass growth transformation symmetrical about the centric seat of all the directions. The experimental procedure to achieve isotropic growth simultaneously in all directions was an inertia of the previously reported work.

2.4. microscopic studies

2.4.1. optical microscopic examination

The microslides of binary organic eutectic composite phases grown anisotropically were examined in a polarizing microscope to view the growth habits of crystallites which during and after the growth, were photographed

2.4.2. electron microscope examination

The metallic specimens grown isotropically and anistropically were polished at room temperature by following the procedure referred in connection with the analogues problem [10]. A thin layer of a specimen etched in ferric chloride was mounted on stub with gold coated holder and examined in a scanning electron microscope (Jeol T-330)

for microgrowth observations. Several experimental samples of eutectic composites were viewed in this manner and growth habits acquired by the growing eutectic phases during solidification process at different growth rates, were photographed.

2.4.3. X-ray diffraction (XRD) studies

X-ray diffraction patterns of eutectics and non-eutectics were scanned in a Rigaku X-ray diffractometer with CuK_{α} radiation of wavelength 1.540A° at room temperature. Both X-ray and thermal analysis are well known complementary techniques that explicitly explore and authenticate the thermal stability, purity, composition, enthalpies of fusion and fusion temperatures of the homogeneous constituent materials, their alloying ability, intermediate products during combination and corresponding liquidus temperatures.

RESULTS AND DISCUSSION

The melting temperatures, enthalpies of fusion and entropies of fusion of homogeneous materials obtained by the experimental techniques mentioned in experimental section are recorded in Table 1. Contrariwise, compositional ratios [7-11] along with the liquidus temperatures of the experimental binary eutectic composite materials are presented in Table 2.

Table 1 : Melting temperatures, enthalpies of fusion, entropies of fusion of homogenous materials

Material	Melting temperature Tm (K)		Enthalpy of fusion ΔH_f (kJ mol^{-1})		Entropy of fusion $\Delta S_f = \Delta H_f / T_m$ (Jmol^{-1}K^{-1})	Dimensionl-ess entropy of fusion $\alpha = \xi\frac{\Delta S_f}{R}$
	Experimental value	Literature value	Experimental value	Literature value		
Naphthalene	353.50	353.26	19.10	19.01	54.03	6.49
Acenaphthene	367.00	367.50	21.00	21.49	57.22	6.88
Benzoic acid	396.00	395.30	18.30	18.20	46.21	5.56
Camphor	449.50	450.00	6.80	6.82	15.13	1.82
Vanillin	354.90	355.00	16.13	16.15	45.47	5.47
Salicylic acid	431.50	432.00	24.62	24.60	57.06	6.86
Camphene	322.70	323	3.08	3.10	9.56	1.15
Cadmium	596.00	596.50	6.19	6.20	10.39	1.25
Bismuth	545.00	545.67	11.20	11.13	20.55	2.47
Tin	509.00	509.12	7.00	7.15	13.75	1.65
Lead	602.00	602.50	4.55	4.77	7.56	0.91

Table 2: Compositional ratios and Liquidus temperatures of binary composite materials

Material	Compositional ratio	Liquidus temperature Tm(K)
tin-Cadmium	72 wt% of Sn, 28 wt% of Cd	450.20
lead-Tin	37 wt% of Pb, 63 wt% of Sn	454.20
lead-Bismuth	58 wt% of Pb, 42 wt% of Bi	410.00
tin-Bismuth	58 wt% of Sn, 42 wt% of Bi	408.20
vanillin-acenapthene	0.6950 molfraction of vanillin 0.3050 molfraction of acenapthene	335.40
naphthalene-acenapthene	0.61 molfraction of naphthalene 0.39 molfraction of acenapthene	326.00
benzoic acid-salicylic acid	0.56 molfraction of benzoic acid 0.44 molfraction of salicyclic acid	385.00
benzoic acid-camphor	0.54 molfraction of camphor 0.46 molfraction of benzoic acid	348.00

The DSC curves resulted in by the thermal analysis of composite alloys Sn-Cd, Pb-Sn, Pb-Bi and Sn-Bi are presented in Fig. 1. (a,b,c,d) explicitly exhibiting their thermal stability, homogeneity and liquidus temperatures. The DSC curves of both nonfaceted-nonfaceted (nf-nf) Pb-Cd and Sn-Zn, and nonfaceted-faceted (nf-f) Cd-Bi, were similar but not exactly the same, to that of Sn-Cd, Pb-Sn, Pb-Bi and Sn-Bi because of the difference in liquidus temperatures.

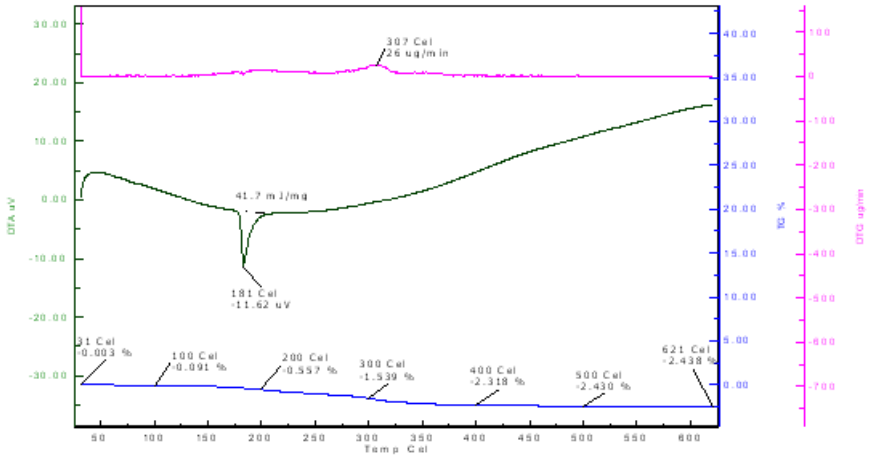
307 Cel
26 ug/min
41.7 mJ/mg
181 Cel
-11.62 uV
31 Cel
-0.003 %
100 Cel
-0.091 %
200 Cel
-0.557 %
300 Cel
-1.539 %
400 Cel
-2.318 %
500 Cel
-2.430 %
621 Cel
-2.438 %
DTA uV
TG %
DTG ug/min
Temp Cel

(a)

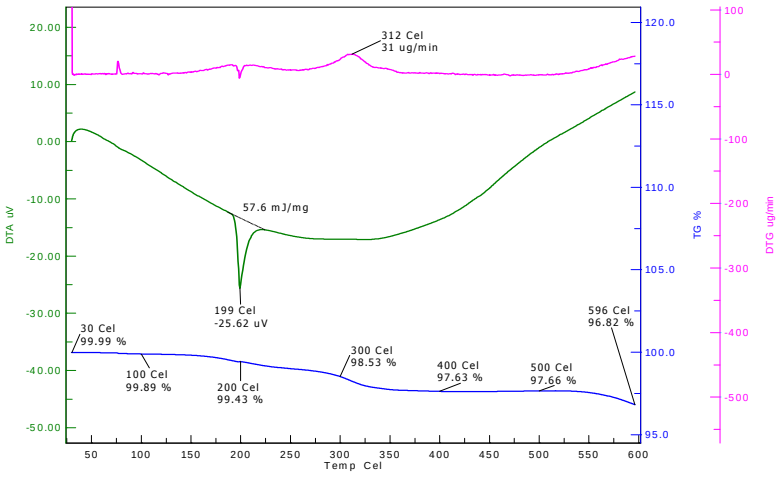
312 Cel
31 ug/min
57.6 mJ/mg
199 Cel
-25.62 uV
30 Cel
99.99 %
100 Cel
99.89 %
200 Cel
99.43 %
300 Cel
98.53 %
400 Cel
97.63 %
500 Cel
97.66 %
596 Cel
96.82 %
DTA uV
TG %
DTG ug/min
Temp Cel

(b)

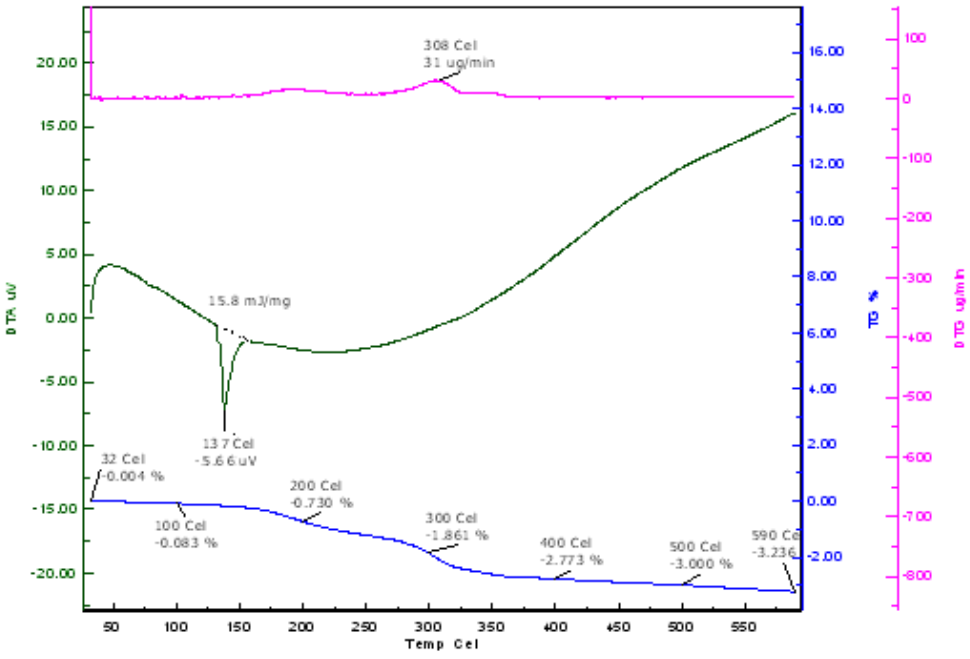
308 Cel
31 ug/min
15.8 mJ/mg
137 Cel
-5.66 uV
32 Cel
-0.004 %
100 Cel
-0.083 %
200 Cel
-0.730 %
300 Cel
-1.861 %
400 Cel
-2.773 %
500 Cel
-3.000 %
590 Cel
-3.236
DTA uV
TG %
DTG ug/min
Temp Cel

(c)

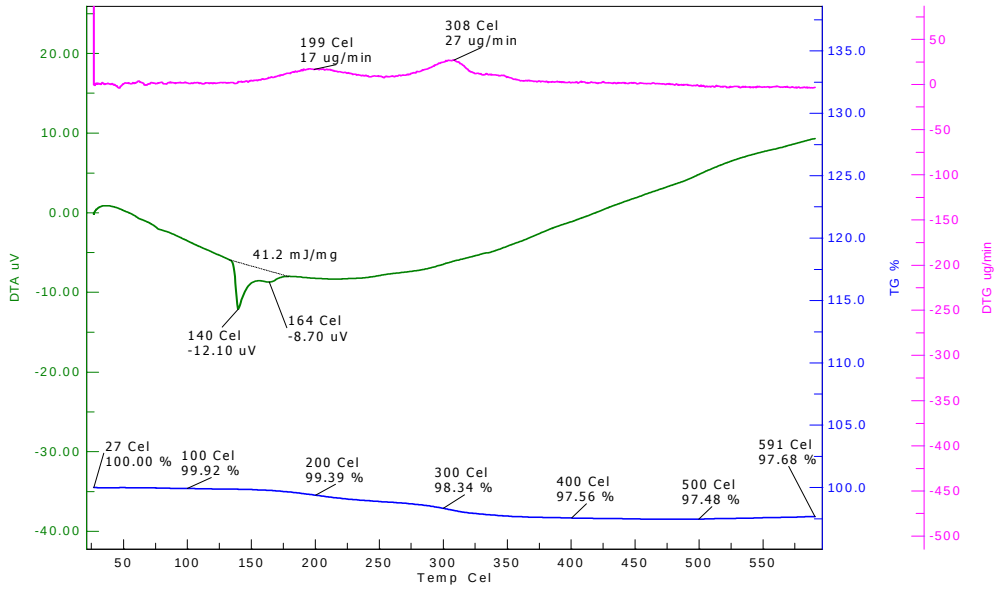

(d)

Fig. 1: DSC curves of composite alloys (a) Sn-Cd; (b) Pb-Sn; (c) Pb-Bi and (d) Sn-Bi

Microscopic studies predict the terminal nature of the eutectic composite alloys which is explicitly confirmed by their X-ray studies. The growth habits of the eutectic phases from the eutectic melts are consentingly found to follow the thermodynamic relation defined in the introduction section. According to the relation, as mentioned earlier, both the eutectic phases have α less than 2 ($\alpha<2$); they essentially grow from the melt isotropically with no crystalline facets transforming the melt into regular crystalline morphology called nonfaceted-nonfaceted (nf-nf) structure. Irregular faceted-faceted (f-f) structure results in when $\alpha > 2$ for both the eutectic phases, which concurrently grow with crystalline facets. Finally, complex regular (nf-f) structure comprises both nonfaceted (nf) and faceted (f) crystals, if one phase has $\alpha<2$ and the other phase is with $\alpha>2$. Succinctly, the regularity being the characteristic feature in the case of nf-nf eutectics is generally lost completely in the case of f-f eutectics. The nf-f eutectics are the intermediate case. The nonfaceted crystal has round growth front, whereas the faceted crystal has a sharp growth front. It is appropriate to mention here that in the nf-nf structure both the eutectic phases grow edgewise producing lamellae or crystallites. The physical understanding of edgewise growth pattern can be visualized from the following theoretical structure of nonfaceted lamellae:

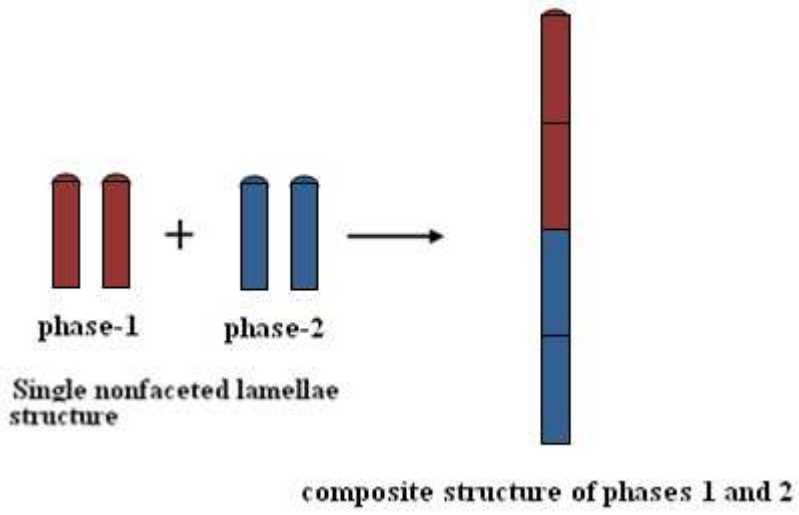

Edgewise (regular growth)

The distribution of the produced lamellae or crystallite in the entirety of their growth structure is completely governed by the microstructural parameters, namely, lamella diameter, lamella length, lamella length distribution, volume fraction of lamellae, and the alignment and packing arrangements of lamellae, expressing their obedience to

the Gauss distribution. In consequence thereof, the spacing among lamellae attains a definite width that would remain constant throughout the structure which appears to be regular. Unlike, both the eutectic phases oftenly grow sidewise in the faceted-faceted structure producing lamellae or crystallites which are of short size, aggressive, disconnected and crossing each other, impelling microstructural parameters to follow the Wiebull distribution. Consequently, the projection of distribution of lamellae or crystallites with variable spacing is termed irregular morphology. The physical significance of the sidewise growth pattern is theoretically predicted in the following:

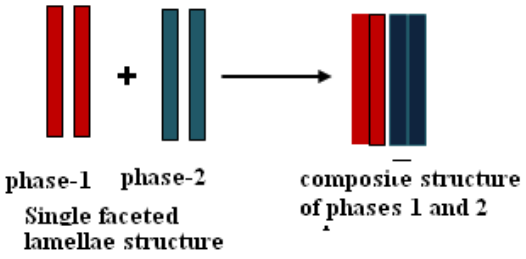

Sidewise (irregular growth)

However the growth habits of the eutectic phases can be structured to non-aggressive, attaching and parallel to each other reinforcing the matrix by anisotropic modes of solidification [12,13]. Finally, the nonfaceted-faceted (nf-f) growth of the eutectic phases acquires complex morphology because of the mixed behaviour of microstructural parameters. Aforementioned types of growth pattern are systematically discussed in the following:

Regular lamellar eutectic Both Phases of the eutectics in this group have low entropies of fusion and grow in a nonfaceted manner. A metallic example (Sn-Cd) is shown in Fig. 2a. Relationships between the growth rate ν, the lamellar spacing λ, and the undercooling at the solidus-liquidus interface ΔT have been measured in lamellar eutectics by other workers [5]. The relationships are $\nu\lambda^2$ = constant and $\Delta T/\sqrt{\nu}$ = constant. Theories have been developed to explain the relationships. Among the assumptions made in the theory, are that both phases grow isotropically with negligible kinetic undercooling and that the eutectic solidus-liquidus interface is isothermal. Experimentally the lamellar spacing of eutectic depends on growth rate. Theoretically, however, for a given lamellar spacing a range of growth rates is possible. It has been proposed that eutectics grow within the stable range with the spacing controlled by the movement of lamellar-faults, which may be explained in the preceding part of discussion. The discontinuous change in spacing in the absence of faults Fig. 3 (a,b and c) is the movement of lamellar-faults, which is an evidence for the fault-mechanism [8-10, 14-20]. It is this movement, not the formation of faults, which is the important factor in controlling the spacing among lamellae. The lamellar cells of homogeneous eutectic phases (Figs. 2c and 3d) would acquire dislocations by virtue of their growth by fault-mechanism from the melt and consequently, exhibit irregular projection. The explanation is self elaboration, why the lamellar structures are less regular, because of lamellar-faults, vis-à-vis rodlike structure (Figs. 2 and 3).

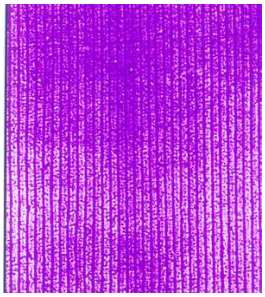

Fig.2(a) Lamellar Sn-Cd eutectic, growth direction from bottom to top at moderate anisotropic growth velocity, 3 x 10^{-7} m^3s^{-1}; magnification 1500 x

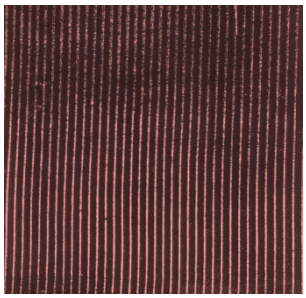

Fig.(b)Lamellar (rodlike) Sn-Pb eutectic, growth direction from bottom to top at moderate anisotropic growth velocity, 3x$10^{-7}$$m^3s^{-1}$; magnification 1500 x

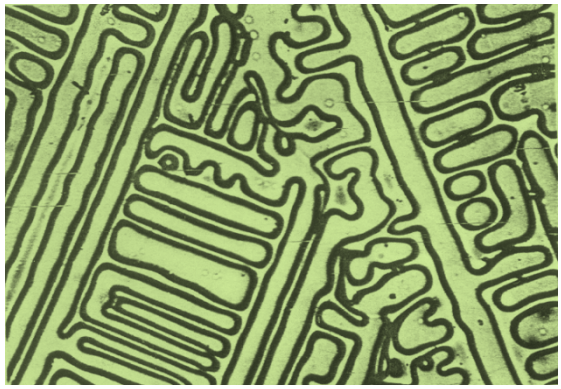

Fig.c Growth pattern of camphene at ~298K; magnification 100 x

Irregular lamellar structure In this group of eutectics, one phase has a high entropy of fusion while the other has a low entropy of fusion. Metallic examples are Al-Si, Pb-Bi, Sn-Bi, Zn-Mg. The authors propose that the structure formed in these alloys is a result of the high kinetic undercooling which is associated with the high entropy of fusion phase.

Irregular structures will be found when the crystal or facet size is of the same size as the eutectic structure.

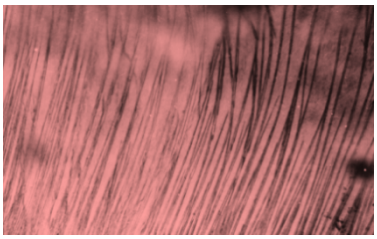

Fig.3(a) Anistropic growth of vanillin-acenaphthene eutectic composite material at growth velocity 3 x 10^{-7} m^3s^{-1}; magnification 100 x

Fig.(b) Anistropic growth of benzoic acid-salicylic acid eutectic composite material at growth velocity 3 x 10^{-7} m^3s^{-1}; magnification 100 x

Fig. (c) Anistropic growth of benzoic acid-camphor eutectic composite material at growth velocity 3 x 10^{-7} m^3s^{-1}; magnification 100 x

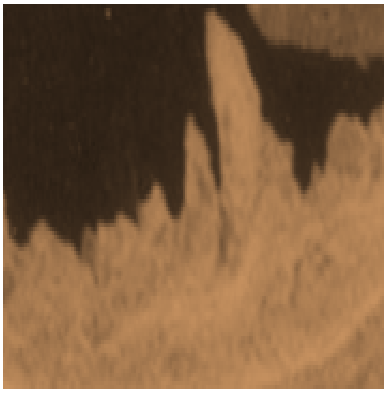

Fig. (d) Microstructure of pure Bi metal (α > 2)at ~298K; magnification 1500 x

Complex regular structure These types of structures are produced over small areas particularly when the alloys are slightly in the faceted component. The authors propose that the structure formed in these alloys is a result of the high kinetic undercooling which is associated with the high entropy of fusion phase. Complex regular structures are sometimes formed in these alloys. This indicates that lamellar formation is possible.

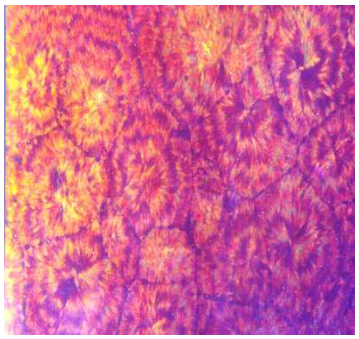

Fig.4(a) Isotropic growth of naphthalene-acenaphthene eutectic composite material in an ice bath (~ 273 K) magnification 100 x.

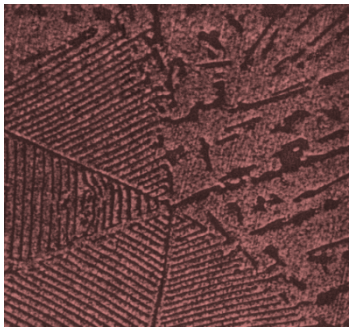

Fig.(b) Anistropic growth of Pb-Bi eutectic composite material at growth velocity 3 x 10^{-7} m^3s^{-1}; magnification 1500 x

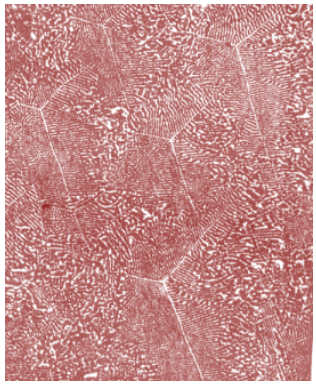

Fig.(c) Anistropic growth of Sn-Bi eutectic composite material at growth velocity 3 x 10^{-7} m^3s^{-1}; magnification 1500 x

Experimental evidences indicate that the nonfaceted-nonfaceted (nf-nf) microstructures of binary eutectic composite materials do exhibit edgewise growth of nonfaceted lamellae of binary constituent phases having α-values less than two (α<2) as illustrated in Figs. 2a and 2b

The homogeneous experimental material Camphene with α less than two (α<2) tends to produce regular solid structure comprising of nonfaceted lamellae (Fig. 2c). A regular structure will therefore only be formed when each lamella of the nonfaceted phase grows as a single-crystal facet and more important when every lamella in the regular region is the same crystal facet.

However, the faceted-faceted (f-f) microgrowth occurs only when both the eutectic phases have α-values greater than two (α>2) and consequently, follows the sidewise growth pattern resulting in an irregular morphologies Fig.

3(a-c). Figure 3 is an experimental confirmation of irregular growth. The homogeneous phase Bi having α-value greater than two (α>2) follows irregular growth wherein the regularity among its growing lamellae is completely lost because of the sidewise growth pattern of the faceted lamellae (Fig. 3d).

Likewise complex regular microstructure (nf-f) appears only when one eutectic phase grows edgewise and the other phase as sidewise. Figure 4(a-c) is an experimental evidence of complex regular growth. In other words, when α-values is low (α<2) in one phase but high (α >2) in other phase, complex regular structures are produced.

The X-rays patterns of composite alloy Sn-Cd, Pb-Sn, Pb-Bi and Sn-Bi represented in Fig. 5 (a,b,c,d) and the XRD data summarized in Table 3 (a,b,c,d) exhibit sharp lines of atomic intensities of their individual constituent phases; i.e. Sn, Cd, Pb and Bi. The analyses of the X-ray data and patterns implicitly, confirms the composite alloys as mechanical mixtures of their constituent phases stimulating weak interactions at atomic levels. This implies that the composite alloys are terminal solidus solutions, since no unique peak or atomic intensity is observed in the analyses[21,22].

(a)

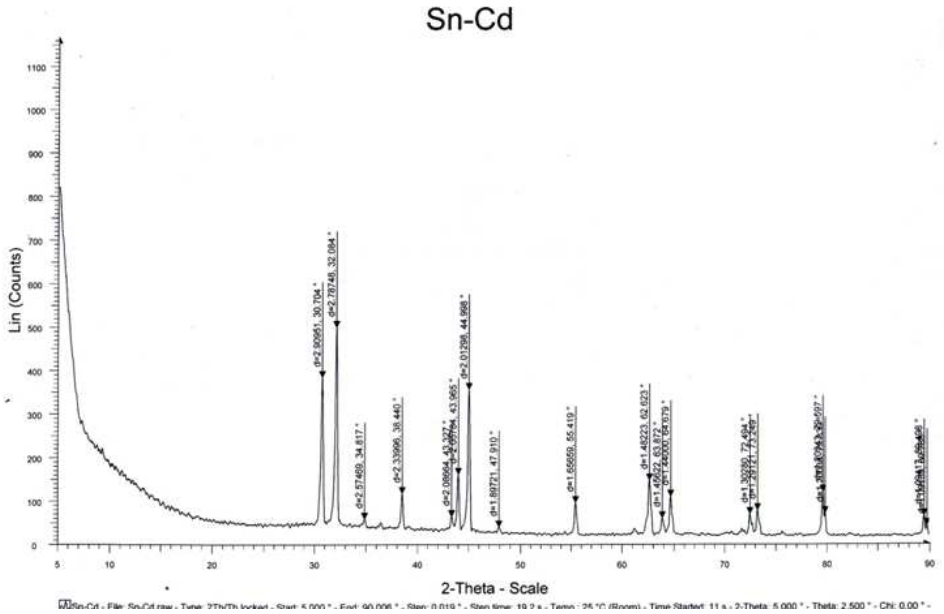

(b)

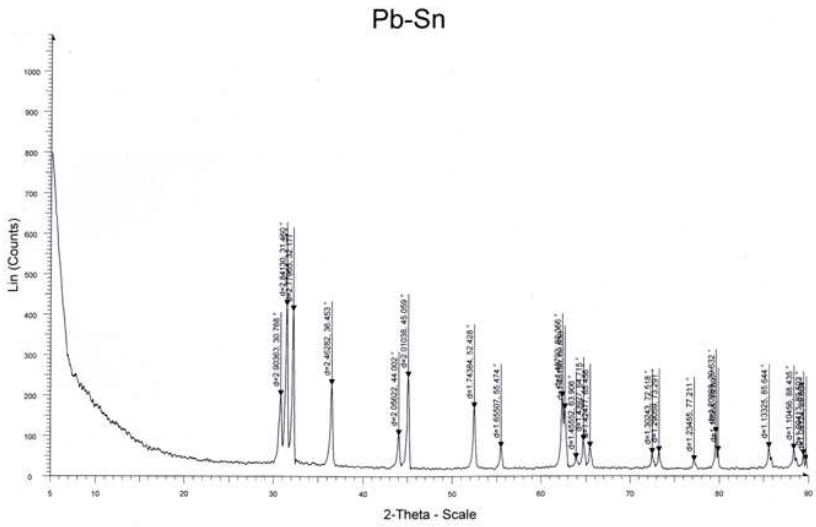

(c)

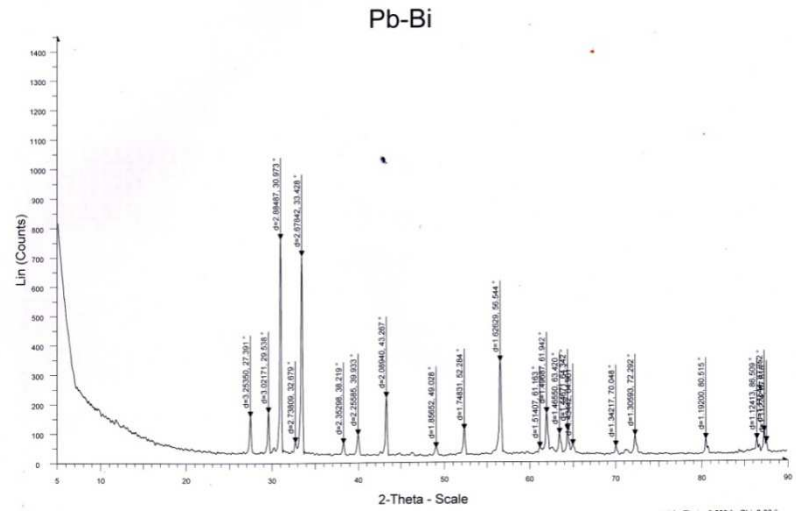

(d)

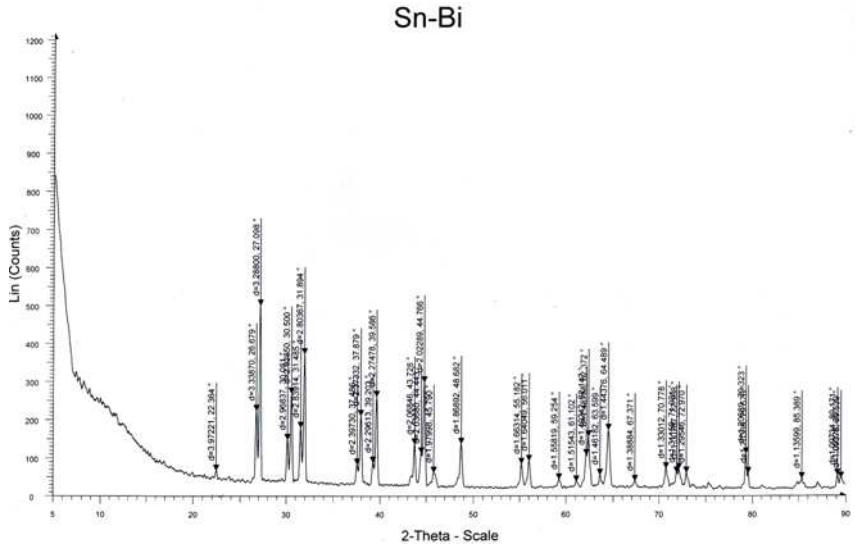

Fig. 5: XRD patterns of composite alloys (a) Sn-Cd, (b) Pb-Sn, (c) Pb-Bi and (d) Sn-Bi

Table 3:XRD data of composite alloys (a) Sn-Cd, (b) Pb-Sn, (c) Pb-Bi and (d) Sn-Bi

(a)

Pos. [2°TH.]	d-spacing [Å]	Intensity [Å]	Intensity [%]	Planes (hkl)
30.704	2.90951	382	76.5	Sn(200)
32.084	2.78748	500	100	Sn(101)
34.817	2.57469	55.8	11.2	Cd(100)
38.440	2.33996	114	22.9	Cd(101)
43.327	2.08664	61.1	12.2	Sn(211)
43.965	2.05784	158	31.7	Sn(220)
44.998	2.01298	355	71.0	Sn(211)
47.910	1.89721	37.1	7.4	Cd(102)
55.419	1.65659	93.0	18.6	Sn(301)
62.623	1.48223	145	28.9	Sn(112)
63.872	1.45622	57.5	11.5	Sn(400)
64.679	1.44000	107	21.4	Sn(321)
72.494	1.30280	66.3	13.9	Sn(420)
73.249	1.29121	74.9	15.0	Cd(200)
79.597	1.20343	117	23.5	Sn(312)
79.839	1.20038	68.1	13.6	Cd(312)
89.498	1.09417	61.7	12.4	Sn(431)
89.788	1.09139	39.9	8.0	Sn(431)

(b)

Pos. [2°TH.]	d-spacing [Å]	Intensity [Å]	Intensity [%]	Planes (hkl)
30.768	2.90363	198	470	Sn(200)
31.460	2.84130	422	100.0	Pb(111)
32.177	2.77965	408	96.8	Sn(101)
36.453	2.46282	225	53.4	Pb(200)
44.002	2.05622	101	23.9	Sn(220)
45.059	2.01038	244	57.8	Sn(211)
52.428	1.74384	168	39.8	Pb(220)
55.474	1.65507	70.9	16.8	Sn(301)
62.356	1.48792	194	46.1	Sn(112)
62.636	1.48190	164	38.9	Sn(112)
63.906	1.45552	41.7	9.9	Sn(400)
64.715	1.43927	86.1	20.4	Sn(321)
65.456	1.42477	69.4	16.4	Pb(222)
72.518	1.30243	53.5	12.7	Sn(420)
73.291	1.29059	58.0	13.7	Sn(420)
77.211	1.23455	36.0	8.5	Sn(312)
79.632	1.20298	105	25.0	Sn(321)
79.897	1.99965	58.6	13.9	Sn(312)
85.644	1.13325	68.1	16.1	Pb(220)
88.435	1.10456	64.0	15.2	Pb(431)
89.502	1.09413	50.1	11.9	Sn(431)
89.804	1.09124	37.5	8.9	Sn(431)

(c)

Pos. [2°TH.]	d-spacing [Å]	Intensity [Å]	Intensity [%]	Planes (hkl)
27.391	3.25350	154	20.3	Bi(012)
29.538	3.02171	168	22.1	Pb(002)
30.973	2.88487	760	100.0	Bi(002)
32.679	2.73809	66.3	8.7	Pb(101)
33.428	2.67842	703	92.5	Bi(101)
38.219	2.35298	61.8	8.1	Bi(104)
39.933	2.25585	90.7	11.9	Bi(110)
43.267	2.08940	218	28.6	Pb(102)
49.028	1.85652	45.1	5.9	Bi(202)
52.284	1.74831	106	14.0	Pb(110)
56.544	1.62629	339	44.6	Pb(103)
61.163	1.51407	44.2	5.8	Bi(205)
61.942	1.49687	161	21.2	Bi(116)
63.420	1.46550	90.6	11.9	Pb(201)
64.342	1.44671	102	13.4	Bi(122)
64.961	1.43442	52.3	6.9	Pb(202)
70.048	1.34217	46.6	6.1	Bi(214)
72.292	1.30593	83.3	11.0	Bi(009)
80.515	1.19200	70.3	9.3	Bi(208)
86.509	1.1241	68.2	9.0	Pb(220)
87.352	1.11544	93.7	12.3	Bi(217)
87.618	1.11274	58.3	7.7	Bi(431)

(d)

Pos. [2°TH.]	d-spacing [Å]	Intensity [Å]	Intensity [%]	Planes (hkl)
22.364	3.97221	165.0	13.0	Bi(003)
26.679	3.33870	222	44.4	Bi(101)
27.098	3.28800	501	100.0	Bi(012)
30.081	2.96837	146	29.1	Bi(100)
30.500	2.92850	268	53.5	Sn(200)
31.485	2.83914	178	35.5	Bi(002)
31.894	2.80367	372	74.2	Sn(101)
37.486	2.39730	81.6	16.3	Bi(104)
37.879	2.37332	209	41.7	Bi(104)
39.203	2.29613	86.3	17.2	Bi(110)
39.586	2.27478	259	51.7	Bi(110)
43.728	2.06846	134	26.7	Sn(110)
44.443	2.03680	111	22.1	Sn(211)
44.766	2.02289	298	59.4	Bi(015)
45.790	1.97998	60.0	12.0	Bi(113)
48.682	1.86892	136	27.1	Bi(202)
55.182	1.66314	82.8	16.5	Sn(301)
56.011	1.64049	90.5	18.0	Bi(103)
59.254	1.55819	41.6	8.3	Bi(107)
61.102	1.51543	35.7	7.1	Bi(205)

62.147	1.49242	106	21.0	Sn(112)
62.372	1.48758	155	30.9	Sn(116)
63.599	1.46182	53.3	10.6	Bi(201)
64.489	1.44376	172	34.3	Sn(321)
67.371	1.38884	37.2	7.4	Bi(018)
70.778	1.33012	701	14.0	Bi(214)
71.931	1.31159	59.2	11.8	Bi(300)
72.168	1.30787	68.6	13.7	Sn(420)
72.970	1.29546	59.0	11.8	Bi(027)
79.323	1.20689	110	21.8	Sn(312)
79.576	1.20369	57.9	11.5	Bi(208)
85.389	1.13599	43.5	8.7	Bi(101)
89.171	1.09734	52.3	10.4	Sn(431)
89.539	1.09378	44.2	8.8	Bi(223)

It is worthwhile to mention here that both the microscopic and the X-ray diffraction studies of eutectic composite materials are complementary to each other in characterizing the solidus structures of the composite phases. The present accomplishment paves the conceptual knowledge for understanding the dependence of physical properties of any composite material on the growth habits of that material.

CONCLUSION

Single-phase materials solidification classifies the binary eutectic composites into three groups, namely, (i) nonfaceted-nonfaceted eutectic structures in which both phases have low entropies of fusion, $\alpha<2$, (ii) faceted-faceted eutectic structures are obtained for those eutectic composites comprising of binary phases which have high entropies of fusion, $\alpha>2$ and (iii) nonfaceted-faceted eutectic structures are characteristics of those eutectic composites in which one phase has a low entropy of fusion $\alpha<2$ and the other phase has a high entropy of fusion, $\alpha>2$. This particular eutectic composite structure is actually the intermediate structure resulting-in from the combination of high and low entropy constituent phases.

Organic eutectics, like the metallic systems, can be classified into three groups, simple lamellar or rodlike structures are only produced in systems where both phases have low entropies of fusion ($\alpha<2$). When the entropy of fusion is low ($\alpha<2$) for one phase but high ($\alpha>2$) for the other, irregular or complex regular structures are produced. When both the phases have high entropies of fusion ($\alpha>2$) regular structures are not produced at all. The three groups are related to the entropy of fusion (α) of the binary eutectic constituent phases.

In the course of present investigation, the evidences were obtained for the following: i) theoretical shape of the lamellar solidus-liquidus interface, ii) the fault-mechanism of lamellar spacing changes, and iii) the formation of a builtup layer during lamellar growth. Direct evidence was obtained for the existence of a low-energy solidus-solidus boundary formed between the lamellae during solidification. A regular structure will therefore, only be formed when each lamella of the nonfacted phase grows as a single crystal facet and more important when every lamella in the regular region is the same crystal facet. An explanation is presented to account for the irregular or complex regular structures formed in the other two eutectic groups.

While, the thermal, microscopic and X-ray diffraction studies of eutectic composite materials authenticate the thermal stability, purity, composition, enthalpies of fusion and melting temperatures of the homogeneous constituent materials, their alloying ability, intermediate products during combination, and liquidus temperature of the condensed phase. These studies further affirm that eutectic composite alloys are mechanical mixtures of their respective constituent phases stimulating weak interactions at atomic levels, indicating them (eutectic alloys) terminal solidus solutions, since no unique peak or atomic intensity is observed in the analyses of eutectic composite materials.

REFERENCES

[1] BL Sharma, Parhotam Lal, Growth Reinforcing Composite Materials from Liquidus Phases: Mecahnical and Microstructural Parameters Relationship Essentially Evincing the Predominance of an Akin Mass Composite over the Domain of Composition, Metal Ceramic and Polymeric Composite for Various uses, John Cuppolettic (Ed.) ISBN:1978-953-307-353-8 In Tech (**2011**).
[2] BL Sharma, S Tandon, S Gupta, *Cryst. Res. Technol*., **2009**, **44**, 258-268.
[3] DE Ovesienko, GA Alfinster, in: T Arizumi (Ed.), Crystal Growth, Properties and Application, *Springer-Verlag, Berlin*, **1980**, **2**.
[4] W Albers, in: H Muller (Ed.), Preprative Methods of Solid State Chemistry, *Academic Press, New York* (**1972**).

[5] JD Hunt, KA Jackson, *Trans. AIME*, **1966**, **236**, 843.
[6] DR Lide, CRC Handbook of Chemistry and Physics, A Ready-References Book of Chemical and Physical Data 90th ed., CRC Press, London (**2009**).
[7] BL Sharma, PS Bassi, NK Sharma, S Kumar, *Composites*, **1989**, **20**, 245.
[8] Arun K Sharma, Parshotam Lal, BK Gondatra, R Kant, BL Sharma, *Arch. Appl. Sci. Res*., **2012**, **4**, 111-127.
[9] CR Tottle, An Encyclopedia of Metallurgy and Materials LXVI, Macdonald and Evans Ltd., Great Britian, (**1984**).
[10] BL Sharma, *J. Alloys Compd.*, **2004**, **385**, 74.
[11] Edward W Washburn, International Critical Tables of Numerical Data, Mc Graw –Hill, New York (**1930**) **VII**, 219.
[12] GR, VD Bhandakkar, BM Suryvanshi, *Arch. Appl. Sci. Res.*, **2012**, **1(1)**, 1-4.
[13] BL Sharma, S Gupta, S Tandon, R Kant, *Mater. Chem. Phys.*, **2008**, **111**, 423-430.
[14] V Renganaki, D Syamala, R Sathyamoorthy, *Arch. Appl. Sci. Res.*, **2012**, 1453-1461.
[15] T Thaila and S Kumarraman, *Arch. Appl. Sci. Res.*, **2012**, 1494-1501.
[16] G Rajaduria, A Puhal Raj, S Pari, *Arch. Appl. Sci. Res.*, **2013**, **5(3)**, 247-253.
[17] Parveen Kumar Nigam, Prabhash Jain, *Arch. Appl. Sci. Res.*, **2013**, **5(1)**, 224-230.
[18] R Josephine Usha, J Arul Martinmani, P Sagayaraj, V Joseph, *Arch. Appl. Sci. Res.*, **2012**, 1545-1552.
[19] R Caram, M Banan, WR Wilcox, *J. Cryst. Growth*, **1991**, **114**, 249.
[20] R Caram, S Chandrasekhar, WR Wilcox, *J. Cryst. Growth*, **1990**, **106**, 294.
[21] BL Sharma, Parshotam Lal, *Arch. Appl. Sci. Res.*, **2012**, **4(5)**, 2244-2255
[22] Parshotam Lal, Shallu Abrol, BL Sharma, *Arch. Appl. Sci. Res.*, **2012**, **5**.